

Jan Degirmendźić University of Lodz, Faculty of Geographical Sciences, Department of Physical Geography  
E-mail: [jan.degirmendzic@geo.uni.lodz.pl](mailto:jan.degirmendzic@geo.uni.lodz.pl)

## Changes in the frequency and persistence of the Vangengeim-Girs macro-circulation forms in the period 1979–2023

### Zmiany częstości oraz czasu trwania makroform Vangengeima-Girsa w latach 1979–2023

#### Abstract

The significantly faster increase in Arctic temperature compared to the global average is causing changes in wind patterns in the mid-latitudes of the upper troposphere. Studies suggest possible changes in the geometry of wind fields, evident in the waviness of geopotential lines or in a series of discrete circulation patterns. This study aligns with the latter research focus. The objective of the analysis is to estimate long-term trends in the Vangengeim-Girs (V-G) macroforms from 1979 to 2023, and since 1999, which is considered a breaking point in the course of Arctic warming.

Trend coefficients were estimated for the 45-year period and in moving 21-year window for characteristics describing V-G forms variability. The results indicate a nonlinear trend in the annual frequency of W and E forms, the number of E episodes, and the duration of C and W episodes. Other parameters maintained a consistent direction of change (+/-) throughout the study period: frequency of C(+), number of W(+), C(+), WEC(+) episodes, duration of WEC(-) and E(-).

Processes indicating an increase in meridionality include the decline in W frequency after 2005, the rise in E frequency after 2003, the increase in C frequency and the number of C episodes from 1979 to 2023, and the rise in the number of E episodes along with a significant decline in W episode duration after 1999.

Additionally, significant trends in the increase (decrease) in the number (duration) of all episodes suggest an increase in day-to-day circulation variability.

#### Keywords

Vangengeim-Girs macro-circulation forms, circulation episodes, long-term trends, Arctic amplification

#### Zarys treści

Wyraźnie szybszy, w porównaniu ze średnią globalną temperaturą, wzrost temperatury Arktyki, powoduje zmiany pola wiatru w szerokościach umiarkowanych w wyższej troposferze. Opracowania wskazują na możliwe zmiany geometrii pola wiatru, widoczne w zafalowaniu pola geopotencjału lub w serii dyskretnych wystąpień układów cyrkulacji. Niniejsze opracowanie wpisuje się w drugi wątek badań. Celem analizy jest oszacowanie wieloletnich trendów makroform Vangengeima-Girsa (V-G) w latach 1979–2023 oraz w okresie od roku 1999, który uznaje się jako rok przełomowy w przebiegu ocieplenia Arktyki.

Oszacowano współczynniki trendów w 45-leciu oraz w ruchomych 21-letnich okresach charakterystyk opisujących zmienność form V-G. Rezultaty wskazują na nieliniowy przebieg częstości rocznych W, E, liczby epizodów E oraz czasu trwania epizodów C i W. Pozostałe parametry utrzymują jednolity kierunek zmian (+/-) przez cały badany okres: częstość C(+), liczba epizodów W(+), C(+), WEC(+), czas trwania WEC(-) i E(-).

Wyróżniono procesy, które wskazują na wzrost przepływu południkowego: spadek częstości formy W po roku 2005, wzrost częstości formy E po roku 2003, wzrost częstości formy C oraz liczby epizodów C w okresie 1979–2023, wzrost liczby epizodów E oraz znaczny spadek czasu trwania epizodów W po roku 1999.

Ponadto istotne trendy: dodatni (ujemny) liczby (czasu trwania) wszystkich epizodów wskazują na wzrost zmienności z dnia na dzień cyrkulacji.

#### Słowa kluczowe

Formy makro-cyrkulacji Vangengeima-Girsa, epizody cyrkulacyjne, wieloletnie trendy, ocieplenie Arktyki.

## 1. Introduction

The significantly faster warming of the Arctic compared to the global average temperature results in a decreasing meridional temperature gradient in the mid-to-high latitudes (Francis and Vavrus 2012; Chylek *et al.* 2022). The processes likely responsible for the accelerated temperature increase in the Arctic are described by Marsz (2023), who also provides numerous references to source

studies. A comprehensive overview of the potential responses of circulation patterns and wind fields associated with Arctic Amplification (AA) is presented by Overland *et al.* (2016). The first stage of climate state transformation, involving the weakening of zonal winds in mid and polar latitudes in the upper troposphere, is fairly well documented (Strong and Davis 2007; Pena-Ortiz *et al.* 2013; Woollings *et al.* 2023). The next stage of changes in the cause-and-effect chain is expected to involve: an increase



in the meridional components of the flow, more frequent occurrences of split flow and blocking highs, the expansion of the ridge in the upper troposphere over the Barents-Kara region, and an increase in the complexity of the flow in the mid-latitudes of the Northern Hemisphere (Overland *et al.* 2016). This stage of changes is continuously being verified. Some authors confirm the presence of the AA signal in wind field variability (Francis and Vavrus 2012; Alizadeh and Lin 2021; Martin 2021; Moon *et al.* 2022; Kornhuber and Messori 2023). Others, such as Blackport and Screen (2020), indicate a complete lack of significant rise in waviness (Local Wave Activity – LWA) in the mid-latitudes of the Northern Hemisphere. The results of some experimental studies also do not confirm the presence of an AA signal in circulation changes (Stewart and Macleod 2022; Schemm and Röthlisberger 2024).

The aim of this analysis is to detect long-term changes in the circulation field defined by the Vangengeim-Girs (V-G) macroforms during the period 1979–2023. To achieve this goal, two types of data were used: (1) the frequency of macroforms, indicating possible shifts in the circulation regime, and (2) the number and persistence of circulation episodes characterizing the intra-annual variability of macroforms. Additionally, it was examined whether, after the year 1999 – identified as the “breaking point” in the AA index series (Chylek *et al.* 2022) – the described trends align with the hypothesis of an “increase in waviness” in the upper troposphere wind field occurring synchronously with Arctic warming.

## 2. Data and methods

The trend analysis utilized time series of Vangengeim-Girs macroform occurrences during the period 1979–2023. Additionally, data covering the first three months of 2024 (JFM) were used. There are three V-G macro-circulation forms identified in the circulation field of the Atlantic-Eurasian sector (between Greenland and the Yenisei River in Eastern Siberia, i.e.  $\sim 40^{\circ}\text{W}$ – $90^{\circ}\text{E}$ ): W – zonal, featuring a small amplitude of long waves; C – meridional, with a large wave amplitude over Europe and a deep trough at 500 hPa over the Ural Mountains; and E – meridional, with a trough over western and central Europe (Sepp 2005; Sidorenkov and Orlov 2008). The 1979–2005 data were obtained from Dimitrieev and Belyazo (2006). Data for 2006–2024 were obtained from the Arctic and Antarctic Research Institute in St. Petersburg (Russia), thanks to the courtesy of Prof. A.A. Marsz (personal communication, 2024). All gaps in the time series were filled using paper-based studies from the aforementioned sources. February 29<sup>th</sup> was excluded from the analysis. It was assumed that the V-G circulation forms calendar was properly compiled and that the published series are homogeneous. Positive assessments regarding the quality of these data were expressed by Sepp (2005, p. 35) and Marsz (2013, p. 10). Nevertheless, it should be noted that subjective classification, developed by various authors over many years, cannot unconditionally guarantee time series ho-

mogeneity. The Hess-Brezowsky classification may serve as an example (e.g. Huth *et al.* 2010; Kucerova *et al.* 2017).

Three characteristics were used in this study: the annual number of macroforms ( $f_w$ ,  $f_e$ ,  $f_c$ ), the annual number of episodes with a given macroform ( $n_{CE_w}$ ,  $n_{CE_e}$ ,  $n_{CE_c}$ ) – where the symbol CE stands for “circulation episode” – and the average annual duration of episodes for a given macroform, referred to as “persistence” ( $d_{CE_w}$ ,  $d_{CE_e}$ ,  $d_{CE_c}$  – the letter “d” denotes duration). An episode is defined as a series of consecutive days with the same circulation form. Episodes were assigned to a given year X if they began in year X. Episodes that continued through the last day of the year and into the following year (X+1) were also assigned to year X (the year in which the episode began). For example, a W macroform episode (29.12.2021–8.01.2022) was assigned to 2021, even though the major part of this episode occurred in 2022. According to the applied rule, this episode was not reassigned to 2022. The average annual number and duration of episodes were calculated from all episodes assigned to a given year. The proposed procedure is simplified compared to the one previously applied by Degirmendžić and Kożuchowski (2019). In that study, the authors assigned a given episode to the year in which the longer part of the episode occurred. Both methods yield nearly identical results: the correlation coefficients between the series of annual nCE (episodes W, E, C, and WEC combined) during the period 1979–2010 (the overlapping period in both studies) range between 0.96 and 0.99.

Linear trend coefficients for the 45-year time series of  $f_{V-G}$ , nCE, and dCE, as well as 21-year moving trends, were estimated. The statistical significance of the trend coefficients was determined using a two-sided t-Student test. Additionally, the standard error of the slope was calculated for the coefficients describing changes over the entire period from 1979 to 2023, according to the formula  $SE(b_1) = b_1/t$ , where SE is the standard error of the slope coefficient  $b_1$  and  $t$  is the Student’s t-statistic (Montgomery *et al.* 1990).

## 3. Annual frequencies of V-G macroforms

The linear trend coefficients for the annual frequencies of V-G circulation macroforms are statistically significant at the 0.05 level. The linear trends explain between 11% and 19% of the total variability in the 45-year series and indicate an increase in the number of days within a year with the W and C macroforms, which implies a decrease in the frequency of the E macroform. However, it should be noted that the nature of the changes in  $f_w$  and  $f_e$  is clearly nonlinear. The W macroform frequency series shows a maximum in 2005, according to the 7-year moving average (Fig. 1), while the annual frequency record for E shows a minimum in the same year (Fig. 2). To describe the nonlinear course of these series, trend coefficients were calculated for 21-year moving bases. Figure 4 presents the results of this analysis. The trends in annual

W frequencies change from positive to negative in 2004–2005 and become statistically significant in later years, indicating a clear decrease in their number after 2005. The trends in annual E frequencies turn positive at the point of transition through 0 between 2000 and 2003. After 2003, a slight increase in positive trend coefficients is observed. However, it should be noted that statistical significance at the 0.05 level is not achieved during the “positive coefficient” period. The trends for the C macroform series cross the 0 value twice, meaning they do

not definitively change sign during the study period, nor do they show statistical significance. The changes in this macroform can be approximated by an increasing linear trend, although this trend halted between 1994 and 2009, as seen in the 7-year moving average in Fig. 3. In summary, starting from 2005, there is a clear decrease in the number of days with the zonal W circulation form, accompanied by an increase in the frequency of the E macroform. The increasing trend in the frequency of the C macroform can be observed throughout the entire 1979–2023 period.

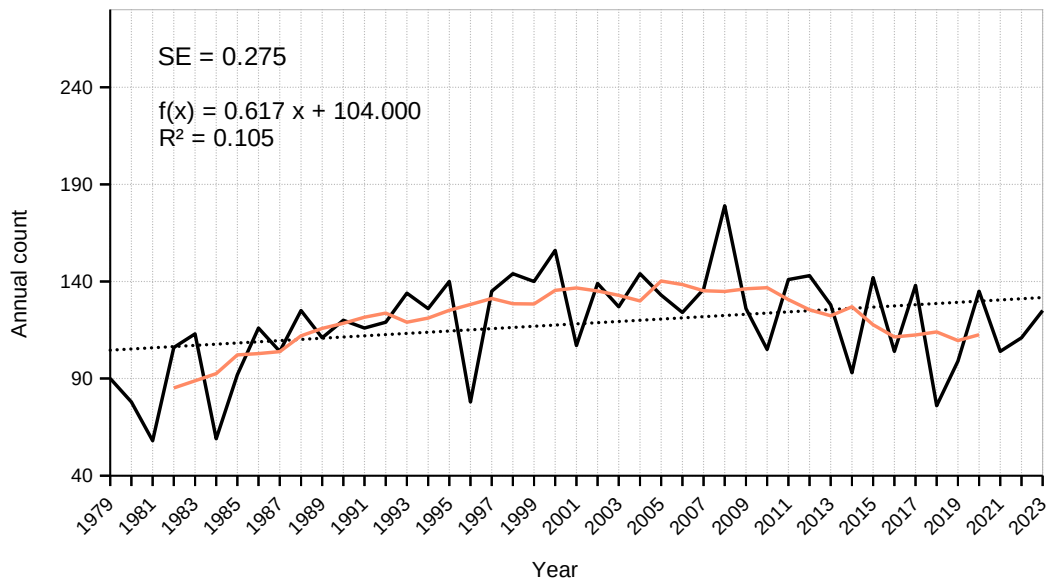


**Fig. 1.** The annual number of W macroform (black line). The trend line (dotted black line), regression equation,  $R^2$ , standard error of the slope coefficient (SE) and 7-year moving average (red line) have been added

**Rys. 1.** Roczna liczba makroformy W (linia czarna). Dodano linię trendu (linia kropkowa), równanie regresji,  $R^2$ , błąd standardowy współczynnika trendu (SE) oraz 7-letnią średnią ruchomą (linia czerwona)

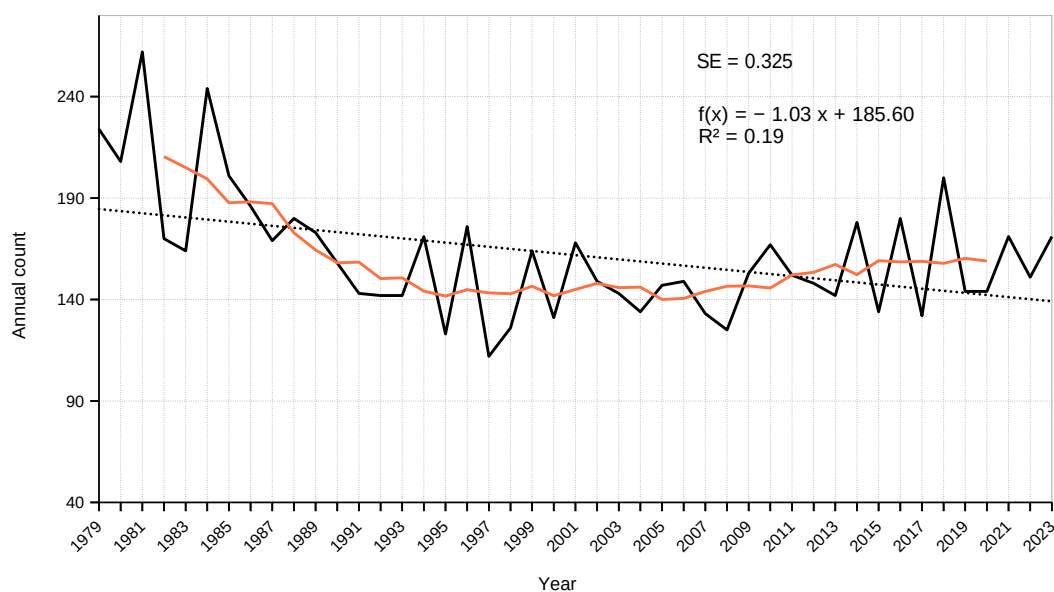


**Fig. 2.** The annual number of E macroform (black line). The trend line (dotted black line), regression equation,  $R^2$ , standard error of the slope coefficient (SE) and 7-year moving average (red line) have been added

**Rys. 2.** Roczna liczba makroformy E (linia czarna). Dodano linię trendu (linia kropkowa), równanie regresji,  $R^2$ , błąd standardowy współczynnika trendu (SE) oraz 7-letnią średnią ruchomą (linia czerwona)

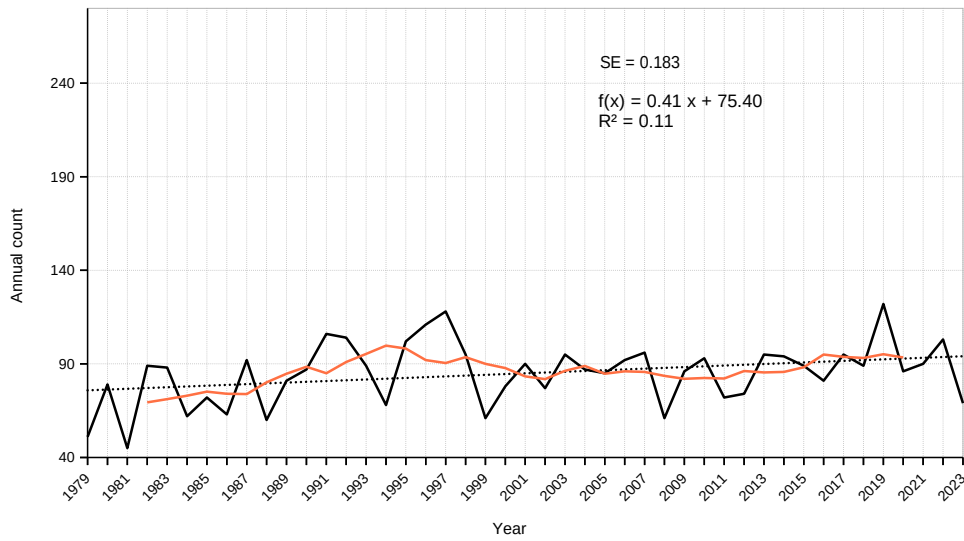


**Fig. 3.** The annual number of C macroform (black line). The trend line (dotted black line), regression equation,  $R^2$ , standard error of the slope coefficient (SE) and 7-year moving average (red line) have been added

**Rys. 3.** Roczna liczba makroformy C (linia czarna). Dodano linię trendu (linia kropkowa), równanie regresji,  $R^2$ , błąd standardowy współczynnika trendu (SE) oraz 7-letnią średnią ruchomą (linia czerwona)

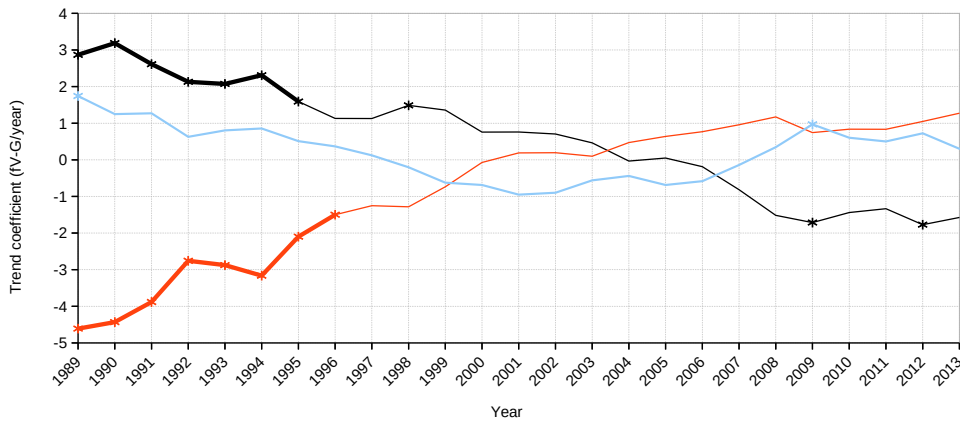


**Fig. 4.** The 21-year moving trend slopes for the annual number of V-G macroforms ( $f_{V-G}$ ): W (black line), E (red line), and C (blue line). Significant coefficients at the 0.05 level are denoted with bold lines and asterisks. The X-axis labels indicate the center of the moving interval

**Rys. 4.** Współczynniki 21-letniego ruchomego trendu rocznych częstości makroform V-G ( $f_{V-G}$ ): W (linia czarna), E (linia czerwona) oraz C (linia niebieska). Istotne współczynniki na poziomie 0.05 zaznaczono pogrubioną linią oraz gwiazdką. Etykiety osi X oznaczają lata środkowe ruchomej podstawy trendu

In the earlier period, i.e., before the change in the sign of the moving trends, statistically significant decreases in the number of E macroforms and increases in the number of W macroforms were observed (Fig. 4).

The moving trends indicate the nonlinearity of changes and a shift in the circulation regime in the mid-troposphere, characterized by a renewed increase in the dominance of the E form over the W form starting from 2007, as indicated by the 7-year moving average (Fig. 5). A significant dominance of the E macroform over W was maintained from 1979, as well as in earlier years, as indicated by the work of Degirmendzić and Kożuchowski (2019). Subsequently, during the period around 1999–2007, the frequencies of both macroforms remained at very simi-

lar levels (Fig. 5). The decrease in the W form's frequency starting from 2005, along with the increase in the C form's frequency, results in their annual frequencies becoming similar to each other. A similar situation occurred in the early years of the study period (Fig. 5).

The above observations confirm a shift in the circulation regime towards a greater dominance of the meridional E macroform over the zonal W form during the years classified as the so-called “low-ice phase” (2007–2016), a period during which minimal Arctic sea ice extent was observed in September (Wang *et al.* 2024). At the same time, the dominance of the W form over the C form decreases, further complementing the description of the aforementioned direction of changes in the circulation regime.

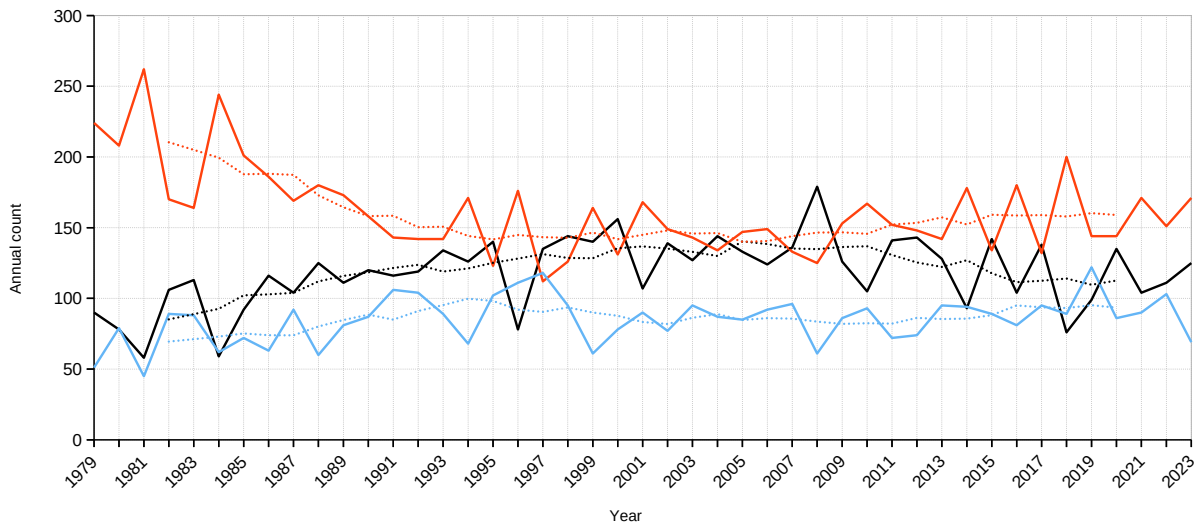


**Fig. 5.** The annual number of W (black line), E (red line), and C (blue line) macroforms in the period 1979–2023. The dotted lines mark 7-year moving average

**Rys. 5.** Roczna częstość makroformy W (linia czarna), E (linia czerwona) i C (linia niebieska) w okresie 1979–2023. Dodano 7-letnią średnią ruchomą (linie kropkowe)

#### 4. Number of circulation episodes

Throughout the entire study period, there is a consistent increase in the number of W and C form episodes (Fig. 6 and 7). The trend coefficients for the period 1979–2023, along with their p-values, summarized in Table 1, indicate the high significance of these changes. The 21-year moving trends remain positive in each sub-period. The only exception is the year 1992, where the 21-year period centered on this year shows a slight negative slope in the trend line for C episodes (Fig. 8).

**Table 1.** Trend coefficients of the annual number of W, E, C, and all episodes (nCE/year) for the period 1979–2023. P-values of the trend's slope and their standard errors (SE) are also included

**Tabela 1.** Współczynniki trendu rocznej liczby epizodów formy W, E, C oraz wszystkich epizodów łącznie (nCE/rok) w okresie 1979–2023 oraz ich istotność statystyczna i błędy standardowe (SE)

	W	E	C	All episodes
p-value	0.002	0.093	0.001	0.000
Slope	0.153	0.063	0.118	0.334
SE	0.045	0.037	0.034	0.088

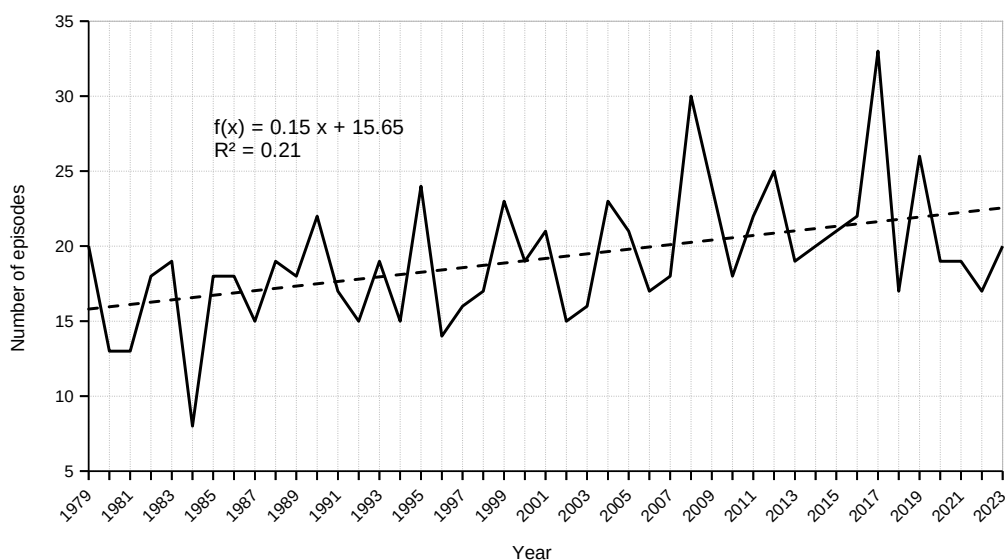


**Fig. 6.** The annual number of W episodes in the period 1979–2023 (solid line). A linear trend with the equation and R<sup>2</sup> is added (dashed line)

**Rys. 6.** Roczna liczba epizodów W w latach 1979–2023 (linia ciągła). Dodano linię trendu (linia przerywana), równanie regresji oraz współczynnik R<sup>2</sup>



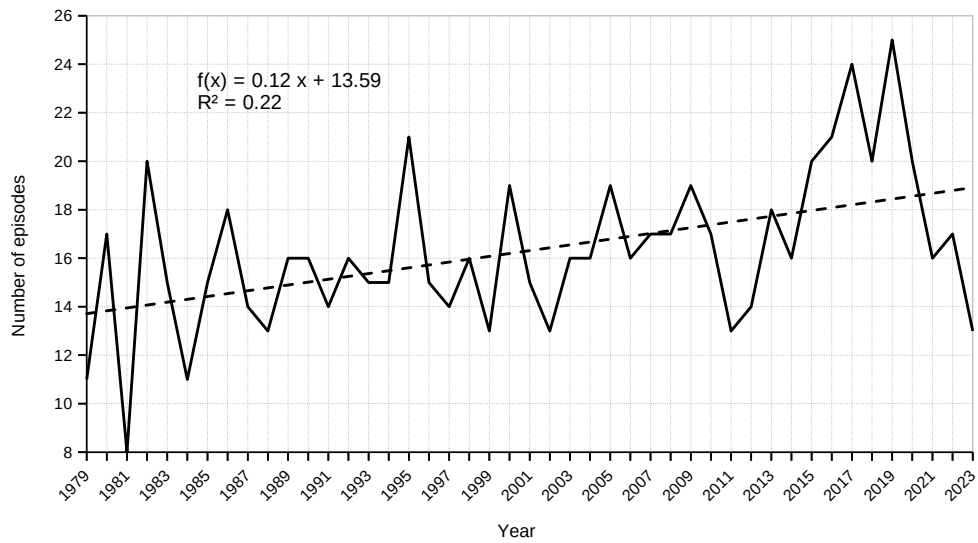


**Fig. 7.** The annual number of C episodes in the period 1979–2023 (solid line). A linear trend (dashed line) with the equation and  $R^2$  is added

**Rys. 7.** Roczna liczba epizodów C w latach 1979–2023 (linia ciągła). Dodano linię trendu (linia przerywana), równanie regresji oraz współczynnik  $R^2$

Episodes of the E macroform exhibit nonlinear changes, with an increase in their number observed only from the year 2000, as indicated by both the 7-year moving average (Fig. 9) and the 21-year moving trends (Fig. 8). It is worth mentioning that the trend's slope for  $nCE_E$ , after crossing through 0, achieves statistical significance over a relatively long period (2005–2011) (Fig. 8). This increase is synchronized with the rising trend in the number of E macroforms, as expressed by the moving trends, which clearly exceed the value of 0 from around 2003 (Fig. 4). The simultaneous occurrence of  $f_E$  and  $nCE_E$  trends with the same sign in the second half of the study

period (ca. 2001–2023) indicates that there is no amalgamation of “additional” days with the E form to create longer series of uninterrupted E circulation. This observation is important in the context of reports suggesting an increase in the frequency and duration of meridional patterns (including blocking patterns) with ongoing Arctic warming (Overland and Wang 2010; Hanna *et al.* 2016). A similar pattern of changes applies to the C form, whose annual frequency increases over the multi-year period, along with a simultaneous increase in the number of episodes. A detailed analysis of episode duration is presented in Section 5.

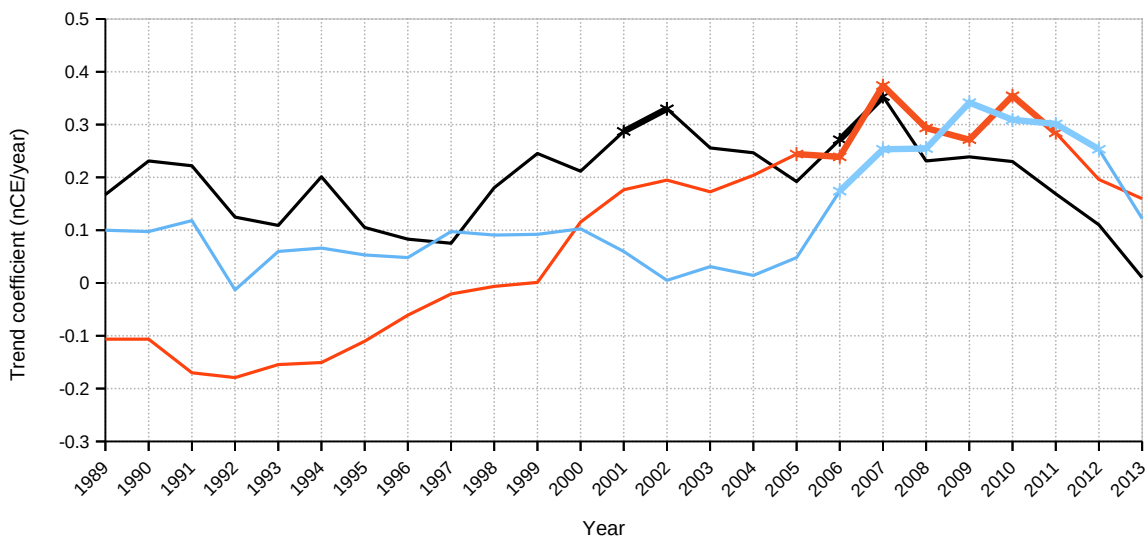


**Fig. 8.** The 21-year moving trend slopes for the annual number of W (black line), E (red line), and C (blue line) episodes. Significant coefficients are marked with bold lines and asterisks

**Rys. 8.** Współczynniki 21-letniego ruchomego trendu rocznych liczebności epizodów: W (linia czarna), E (linia czerwona) oraz C (linia niebieska). Istotne współczynniki na poziomie 0.05 zaznaczono pogrubioną linią oraz gwiazdką

It is worth emphasizing, in the context of ongoing Arctic Amplification, that only in the second half of the analyzed period (2001–2023) do the observed increases in  $nCE_W$  and  $nCE_C$  achieve statistical significance. Additionally, during these years, the  $nCE_E$  parameter also begins to rise and reaches statistical significance (Fig. 8). Thus, after 1999 (“breaking point” in the course of AA), a general trend of increasing the frequency of day-to-day changes in V-G macroforms can be observed.

The most significant trend characterizing the variability of V-G macroforms is the increase in the number of circulation episodes of all macroforms within a year (Fig. 10). The slope of the regression line suggests an average increase of slightly more than 3 episodes per decade. The linear trend explains approximately  $\frac{1}{4}$  of the variability in the series. With the number of days in a year remaining constant, such a marked increase in  $nCE_{WEC}$  must be associated with a decrease in the average duration of an episode.

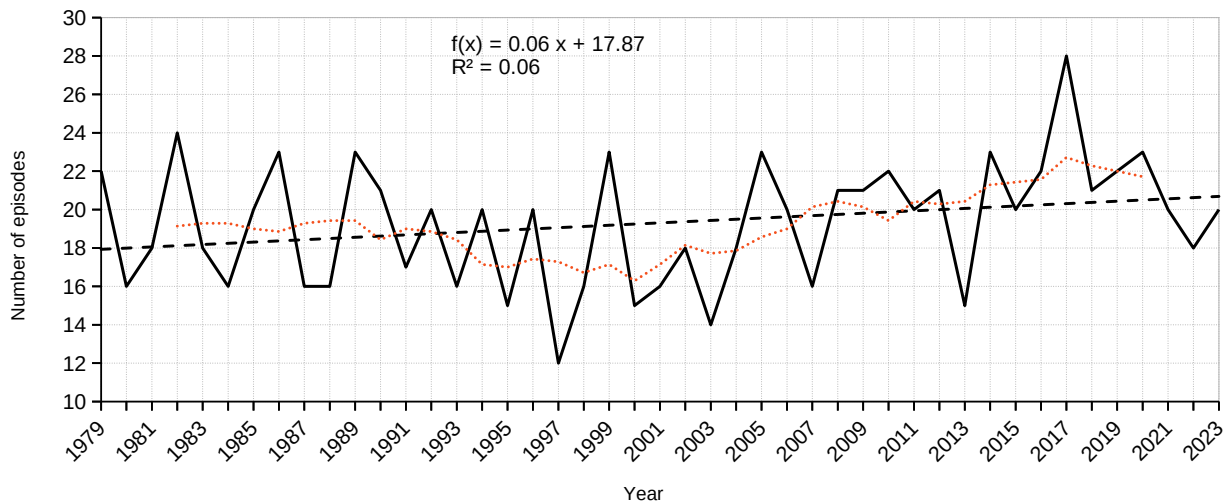


**Fig. 9.** The annual number of E episodes in the period 1979–2023 (solid line). A linear trend (dashed line) with the equation,  $R^2$  and 7-year moving average are added (dotted red line)

**Rys. 9.** Roczna liczba epizodów E w latach 1979–2023 (linia ciągła). Dodano linię trendu (linia przerywana), równanie regresji, współczynnik  $R^2$  oraz 7-letnią średnią ruchomą (linia kropkowa)

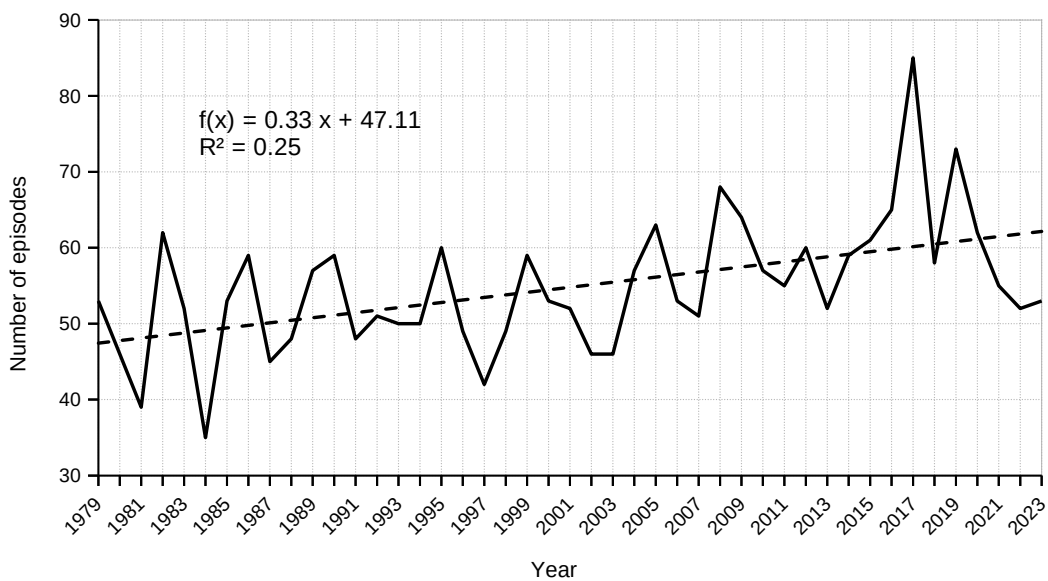


**Fig. 10.** The annual number of all (W, E, C) episodes in the period 1979–2023 (solid line). The linear trend (dashed line) with the equation and  $R^2$  is presented

**Rys. 10.** Roczna liczebność wszystkich epizodów łącznie (W, E, C) w latach 1979–2023 (linia ciągła). Dodano linię trendu (linia przerywana), równanie regresji oraz współczynnik  $R^2$

## 5. Persistence of circulation episodes

The average duration of a circulation episode ( $dCE_{WEC}$ ) decreased from approximately 7–8 (7.7) days in the first year of analysis to 5–6 (5.8) days in 2023, according to the linear regression equation (Fig. 11). This means that the average circulation episode shortened by about 2 days over the period 1979–2023.  $R^2 = 0.28$  indicates a significant contribution of the linear decline in the series of annual persistence values. The shortening of the duration of circulation episodes, considered collectively, is primarily due to the negative trend in the persistence of the E macroform, which remained present throughout the entire study period – the coefficients of the 21-year moving trends for  $dCE_E$  never reached positive values (Fig. 13). The E form lasted continuously for about 11 days at the beginning of the multi-year period and less than 8 days at the end of the 1979–2023 period, as indicated by the 7-year moving average values (Fig. 12).

In the second half of the study period, the moving trends in the persistence of all V-G macroforms are negative (Fig. 13). The rate of these declines varies significantly between episodes of the E and C forms compared to the W form. Due to the increasing trend in the annual frequency of the C macroform throughout the entire multi-year period and the E macroform after 2005, the increasing number of episodes of these macroforms is not associated with a marked shortening of their duration (Fig. 12). In fact, it can be observed that the values of  $dCE_C$  and  $dCE_E$  have remained almost unchanged since 2005. However, it is crucial to emphasize that the shortening of the average duration of W episodes is very pronounced. This can be observed both in the 7-year moving average (Fig. 12) and in the 21-year moving trends, which reach distinct negative and statistically significant values starting from 2006 (Fig. 13). This rapid decrease in the persistence of W episodes is clearly due to the increasing number of W episodes, which, along with their decreasing frequency, contributes to the decrease in their persistence. Such a pattern of changes is associated with the fragmentation of W episodes.

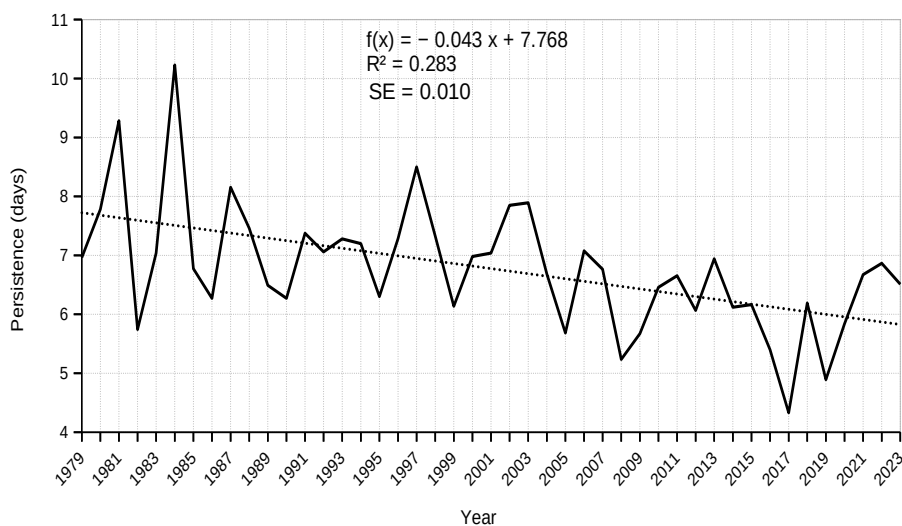


**Fig. 11.** Mean annual persistence of all episodes (W, E, C) in the period 1979–2023 (solid line). A linear trend (dotted line) with the equation,  $R^2$  and standard error (SE) of the slope coefficient is added

**Rys. 11.** Średni roczny czas trwania wszystkich epizodów łącznie (W, E, C) w okresie 1979–2023 (linia ciągła). Dodano linię trendu (linia kropkowa), równanie regresji, współczynnik  $R^2$  oraz błąd standardowy współczynnika trendu (SE)

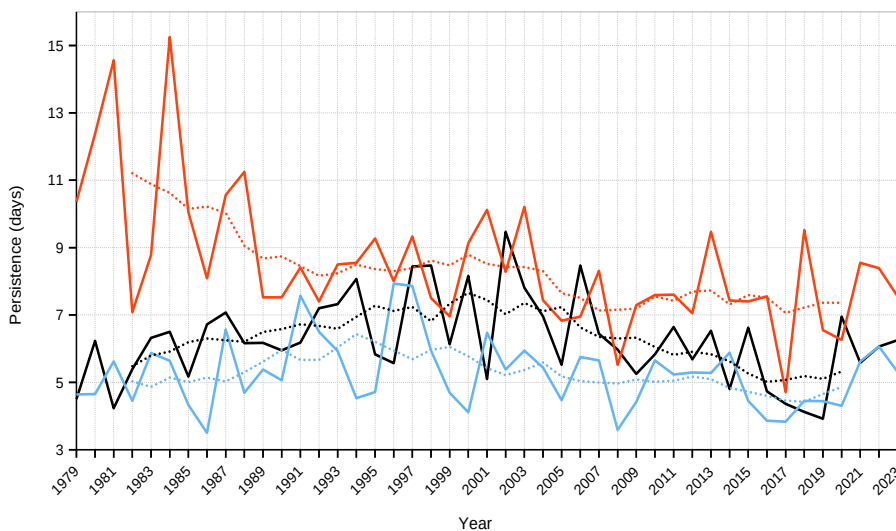


**Fig. 12.** Mean annual persistence of circulation episodes: W (black line), E (red line), and C (blue line) macroforms in the period 1979–2023. The dotted lines mark 7-year moving average

**Rys. 12.** Średni roczny czas trwania epizodów cyrkulacyjnych: W (linia czarna), E (linia czerwona) i C (linia niebieska) w latach 1979–2023. Dodano 7-letnią średnią ruchomą (linie kropkowe)



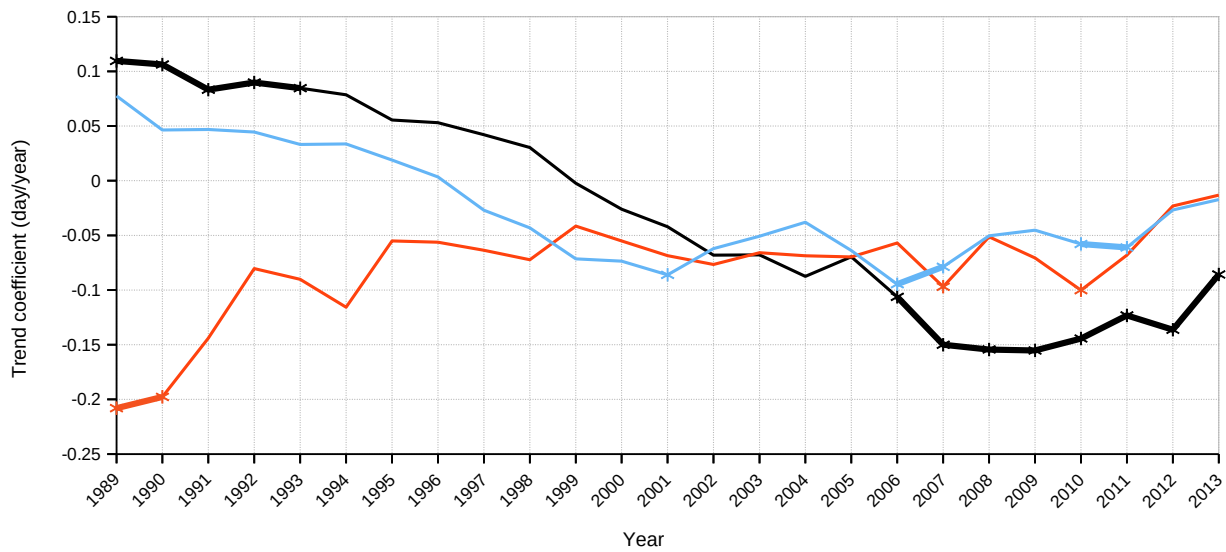


**Fig. 13.** The 21-year moving trend slopes for the mean annual persistence of episodes: W (black line), E (red line), and C (blue line). Significant coefficients at the 0.05 level are marked with bold lines and asterisks

**Rys. 13.** Współczynniki 21-letnich ruchomych trendów średniego rocznego czasu trwania epizodów: W (linia czarna), E (linia czerwona) oraz C (linia niebieska). Współczynniki istotne na poziomie 0.05 zaznaczono pogrubioną linią oraz gwiazdką

### 6. Summary and discussion

The results of the analysis indicate a nonlinear temporal pattern for most of the parameters characterizing the variability of V-G macroforms. The time series for  $f_w$ ,  $f_E$ ,  $nCE_E$ ,  $dCE_C$ , and  $dCE_W$  are characterized by a single change

in the sign of the moving trend during the period 1979–2023. The years in which these trend slopes crossed the 0 value, as well as the signs of the trends before and after this transition year, are summarized in Table 2. It is worth noting that only one characteristic ( $dCE_C$ ) changed its sign before 1999 "breaking year".

**Table 2.** The years of transition through the 0 value of the 21-year moving trends for those V-G characteristics that changed the trend sign only once during the study period. The moving trend basis was centered on the year indicated in the table. The year 1999 is marked as the "breaking point" in the AA series according to Chylek *et al.* (2022) and the "high-ice" (blue) and "low-ice" (green) phases according to Wang *et al.* (2024). Ice phases are bounded by the first and last year representing the center of the moving trends (1989–2013)

**Tabela 2.** Lata przejścia przez wartość 0 21-letnich ruchomych trendów charakterystyk makroform V-G, które tylko raz zmieniły znak trendu w okresie 1979–2023. Ruchomą podstawę trendów wycentrowano na roku podanym w tabeli. Zaznaczono rok 1999 jako „breaking point” w serii AA (Chylek i in. 2022) oraz okresy „high-ice” (nieb.) i „low-ice” (ziel.) według Wang i in. (2024). Ograniczono je krańcowymi latami (1989–2013) stanowiącymi środek ruchomych trendów

Characteristic	1989	1990	1991	1992	1993	1994	1995	1996	1997	1998	1999	2000	2001	2002	2003	2004	2005	2006	2007	2008	2009	2010	2011	2012	2013
$f_w$	+	+	+	+	+	+	+	+	+	+	+	+	+	+	+	0	0	-	-	-	-	-	-	-	-
$f_E$	-	-	-	-	-	-	-	-	-	-	-	0	0	0	0	+	+	+	+	+	+	+	+	+	+
$nCE_E$	-	-	-	-	-	-	-	-	-	-	0	+	+	+	+	+	+	+	+	+	+	+	+	+	+
$dCE_C$	+	+	+	+	+	+	+	0	0	-	-	-	-	-	-	-	-	-	-	-	-	-	-	-	-
$dCE_W$	+	+	+	+	+	+	+	+	+	+	0	-	-	-	-	-	-	-	-	-	-	-	-	-	-

Considering also the parameters that maintained a consistent trend (+ or -) throughout the entire study period (or whose trend's slope changed sign only temporarily and not definitively), namely  $f_c(+)$ ,  $nCE_w(+)$ ,  $nCE_c(+)$ ,  $nCE_{wEC}(+)$ ,  $dCE_{wEC}(-)$ , and  $dCE_E(-)$ , an attempt can be made to classify these processes into two categories: (1) those that align with the anticipated changes in the

state of the climate system, including the circulation field, induced by Arctic Amplification (AA), which, in simplified terms, involves an increase in so-called "waviness" and more frequent occurrences of split flow and blocking patterns (Francis and Vavrus 2015; Overland *et al.* 2016), and (2) other processes that do not confirm such a direction of change.

Category 1 includes the following processes, documented during the course of this analysis:

- (a) a decrease in the annual frequency of the W form after 2005;
- (b) an increase in the annual frequency of the E form after 2003;
- (c) an increase in the annual frequency of the C form during the period 1979–2023;
- (d) an increase in the number of C episodes during the period 1979–2023;
- (e) an increase in the number of E episodes after 1999;
- (f) a significant decrease in the persistence of W episodes after 1999.

As a result of processes 1a and 1b, a dominance of the E form over the W form emerges, starting from 2006. These two processes indicate the definitive end of the WWC epoch (1989–2010), characterized by the dominance of the W form, as identified by Degirmendžić and Kożuchowski (2019).

Category 2 includes two processes:

- (a) an increase in the number of W episodes – although it should be noted that their duration is decreasing;
- (b) a slight decrease in the persistence of C episodes after 1997.

Other highly significant trends, such as the positive trend in the total number of episodes ( $nCE_{WEC}$ ) and the negative trend in the persistence of all episodes ( $dCE_{WEC}$ ), are summary trends (they do not illustrate separate processes) and therefore have not been assigned to any category. These trends undoubtedly indicate an increase in the day-to-day variability of V-G circulation macroforms. The variability of individual macroforms shapes these trends. The linear increase in the number of W and C episodes, as well as the marked increase in the number of E episodes after 2003, along with the trends of shortening the duration of each macroform after 1999, point to faster transitions between successive macroforms. Similar changes in circulation episode parameters were noted by Degirmendžić and Kożuchowski (2019). Based on data up to 2010, the authors observed an increase in the annual number of V-G form alterations ( $nCEs$ ) and a decrease in their persistence. These changes were interpreted as “increasing variability in circulation conditions”. Updated V-G time records indicate the continuation of these trends. A similar transformation of the circulation regime is suggested by Nowosad (2017), who observed a highly significant increase in the standard deviation of the zonal index in Central Europe during the period 1948–2016. Although Nowosad's study analyzes SLP data (sea-level pressure series), it is highly probable that the increasing variability of macro-circulation systems at the 500 hPa level is reflected in fluctuations in the pressure field in the lower troposphere. The relationship between V-G forms and lower pressure systems was confirmed by Marsz (2013) and Kożuchowski and Degirmendžić (2018).

This distinct climate trend, characterized by increasing variability of macro-circulation systems in the mid-troposphere, may suggest a shortening of the Index Cycle

(Barry and Carleton 2001), indicating an accelerated transformation of Rossby waves from a quasi-zonal to a meridional pattern. However, this is presented as a working hypothesis that requires further research and verification.

Finally, it is important to note that the long-term trends in V-G macroform variability analyzed in this study are based on binary data (i.e., the presence or absence of a given circulation form). As such, the time series do not capture subtle changes in the waviness of the flow at the 500 hPa level – changes that are analyzed using continuous (in time and space) geopotential fields and various indices that describe the meandering of the field (e.g., Francis and Vavrus 2015; Di Capua and Coumou 2016; Martin 2021; Alizadeh and Lin 2021). Despite this limitation, the author believes that most of the detected climate trends in the time series of V-G form occurrences are complementary to observations or scenarios of atmospheric circulation changes in the mid-latitudes of the Northern Hemisphere, indicating an increase in the frequency of non-zonal circulation forms during the period of Arctic Amplification.

## 7. References

- Alizadeh O., Lin Z. 2021. Rapid Arctic warming and its link to the waviness and strength of the westerly jet stream over West Asia. *Global and Planetary Change* 199, 103447: 1–11. <https://doi.org/10.1016/j.gloplacha.2021.103447>
- Barry R.G., Carleton A.M. 2001. *Synoptic and dynamic climatology*. Routledge, London and New York: 620 pp.
- Blackport R., Screen J.A. 2020. Insignificant effect of Arctic amplification on the amplitude of midlatitude atmospheric waves. *Science Advances* 6, eaay2880: 1–9. <https://doi.org/10.1126/sciadv.aay2880>
- Chylek P., Folland C., Klett J.D., Wang M., Hengartner N., Lesins G., Dubey M.K. 2022. Annual mean Arctic Amplification 1970–2020: Observed and simulated by CMIP6 climate models. *Geophysical Research Letters* 49, e2022GL099371: 1–8. <https://doi.org/10.1029/2022GL099371>
- Degirmendžić J., Kożuchowski K. 2019. Variation of macro-circulation forms over the Atlantic-Eurasian temperate zone according to the Vangengeim-Girs classification. *International Journal of Climatology*: 1–15. <https://doi.org/10.1002/joc.6118>
- Di Capua G., Coumou D. 2016. Changes in meandering of the Northern Hemisphere circulation. *Environmental Research Letters* 11, 094028: 1–9. <https://doi.org/10.1088/1748-9326/11/9/094028>
- Dimitriev A.A., Belyazo V.A. 2006. *Kalendarnyj katalog atmosferynykh processov po cirkumpolarnoj zonie severnogo polushariya i ikh kharakteristiki za period s 1949 po 2005 g* (Calendar catalogue of atmospheric processes in the Northern Hemisphere circumpolar zone and their characteristics in the period 1949–2005), [w:] *Kosmos, Planetarnaya Klimaticheskaya Izmenchivost' i Atmosfera Polarnykh Regionov*. St. Petersburg: Gidrometeoizdat: 358 pp. (in Russian).
- Francis J.A., Vavrus S.J. 2012. Evidence linking Arctic amplification to extreme weather in mid-latitudes. *Geophysical Research Letters* 39, L06801: 1–6. <https://doi.org/10.1029/2012GL051000>
- Francis J.A., Vavrus S.J. 2015. Evidence for a wavier jet stream in response to rapid Arctic warming. *Environmental Research Letters* 10, 014005: 1–12. <https://doi.org/10.1088/1748-9326/10/1/014005>
- Hanna E., Cropper T.E., Hall R.J., Cappelen J. 2016. Greenland Blocking Index 1851–2015: A regional climate change signal. *International Journal of Climatology* 36: 4847–4861. <https://doi.org/10.1002/joc.4673>

- Huth R., Cahynova M., Kysely J. 2010. The Hess and Brezowsky synoptic catalogue: A timeless concept (although with a few drawbacks). EMS Annual Meeting Abstracts 7, EMS2010-733, 10<sup>th</sup> EMS/8<sup>th</sup> ECAC.
- Kornhuber K., Messori G. 2023. Recent Increase in a Recurrent Pan-Atlantic Wave Pattern Driving Concurrent Wintertime Extremes. *Bulletin of the American Meteorological Society* 104: 1694–1708. <https://doi.org/10.1175/BAMS-D-21-0295.1>
- Kożuchowski K., Degirmendžić J. 2018. Zmienność form cyrkulacji śródkowotroposferycznej według klasyfikacji Wangenheima-Girsa i ich relacje z polem ciśnienia na poziomie morza. *Przegląd Geofizyczny LXIII* (1–2): 89–122.
- Kučerová M., Beck C., Philipp A., Huth R. 2017. Trends in frequency and persistence of atmospheric circulation types over Europe derived from a multitude of classifications. *International Journal of Climatology* 37: 2502–2521. <https://doi.org/10.1002/joc.4861>
- Marsz A.A. 2013. Frekwencja makrotypów cyrkulacji śródkowotroposferycznej według klasyfikacji Wangengejma-Girsa w okresie zimowym a pole ciśnienia atmosferycznego nad Europą i północną Azją. *Przegląd Geofizyczny* 58: 3–23.
- Marsz A.A. 2023. Wewnętrzny mechanizm zmienności i zmian klimatu. *Stowarzyszenie Klimatologów Polskich*, Reda–Warszawa: 279 pp.
- Martin J.E. 2021. Recent trends in the waviness of the Northern Hemisphere wintertime polar and subtropical jets. *Journal of Geophysical Research: Atmospheres* 126, e2020JD033668: 1–15. <https://doi.org/10.1029/2020JD033668>
- Montgomery D.C., Peck E.A., Vining G.G. 1990. Introduction to linear regression analysis. *Wiley Series in Probability and Statistics*, New York: 872 pp.
- Moon W., Kim B.-M., Yang G.-H., Wettlaufer J.S. 2022. Wavier jet streams driven by zonally asymmetric surface thermal forcing. *Proceedings of the National Academy of Sciences USA* 119, e2200890119: 1–8. <https://doi.org/10.1073/pnas.2200890119>
- Nowosad M. 2017. Variability of the zonal circulation index over Central Europe according to the Litynski method. *Geographia Polonica* 90: 417–430. <https://doi.org/10.7163/GPol.0111>
- Overland J.E., Wang M. 2010. Large-scale atmospheric circulation changes are associated with the recent loss of Arctic sea ice. *Tellus* 62A: 1–9. <https://doi.org/10.1111/j.1600-0870.2009.00421.x>
- Overland J.E., Dethloff K., Francis J.A., Hall R.J., Hanna E., Kim S.-J., Screen J.A., Shepherd T.G., Vihma T. 2016. Nonlinear response of mid-latitude weather to the changing Arctic. *Nature Climate Change* 6: 992–999. <https://doi.org/10.1038/NCLIMATE3121>
- Pena-Ortiz C., Gallego D., Ribera P., Ordóñez P., Alvarez-Castro M.D.C. 2013. Observed trends in the global jet stream characteristics during the second half of the 20<sup>th</sup> century. *Journal of Geophysical Research: Atmospheres* 118: 2702–2713. <https://doi.org/10.1002/jgrd.50305>
- Schemm S., Röthlisberger M. 2024. Aquaplanet simulations with winter and summer hemispheres: Model setup and circulation response to warming. *Weather and Climate Dynamics* 5: 43–63. <https://doi.org/10.5194/wcd-5-43-2024>
- Sepp M. 2005. Influence of atmospheric circulation on environmental variables in Estonia. *Dissertationes Geographicae Universitatis Tartuensis* 25: 84.
- Sidorenkov N.S., Orlov I.A. 2008. Atmospheric circulation epochs and climate changes. *Russian Meteorology and Hydrology* 33: 553–559. <https://doi.org/10.3103/S1068373908090021>
- Stewart K.D., Macleod F. 2022. A laboratory model for a meandering zonal jet. *Journal of Advances in Modeling Earth Systems* 14, e2021MS002943: 1–24. <https://doi.org/10.1029/2021MS002943>
- Strong C., Davis R.E. 2007. Winter jet stream trends over the Northern Hemisphere. *Quarterly Journal of the Royal Meteorological Society* 133: 2109–2115. <https://doi.org/10.1002/qj.171>
- Wang Y., Yang Y., Huang F. 2024. Cold Air Outbreaks in Winter over the Continental United States and Its Possible Linkage with Arctic Sea Ice Loss. *Atmosphere* 15: 1–14. <https://doi.org/10.3390/atmos15010063>
- Woollings T., Drouard M., O'Reilly C.H., Sexton D.M.H., McSweeney C. 2023. Trends in the atmospheric jet streams are emerging in observations and could be linked to tropical warming. *Communications Earth & Environment* 4(125): 1–8. <https://doi.org/10.1038/s43247-023-00792-8>